Original Paper

Early View publication on www.interscience.wiley.com (issue and page numbers not yet assigned; citable using Digital Object Identifier – **DOI**)

phys. stat. sol. (a), 1–7 (2007) / **DOI** 10.1002/pssa.200622399

Ferroelectric $BaTiO_3$ nanoceramics prepared by a three-step high-pressure sintering method

C. J. Xiao[1], **W. W. Zhang**[1], **Z. H. Chi**[1], **F. Y. Li**[1], **S. M. Feng**[1], **C. Q. Jin**[*, 1], **X. H. Wang**[2], **L. T. Li**[2], and **R. Z. Chen**[2]

[1] Institute of Physics, Chinese Academy of Science, Beijing 100080, P.R. China
[2] Department of Materials Science and Engineering, Tsinghua University, Beijing 100084, P.R. China

Received 5 July 2006, revised 14 September 2006, accepted 10 October 2006
Published online 22 January 2007

PACS 61.10.Nz, 77.84.Dy, 81.07.Bc, 81.20.Ev

Dense $BaTiO_3$ nanoceramics with a homogeneous grain size of 30 nm were prepared at 6 GPa, 1000 °C using a three-step high-pressure sintering method. The microstructure of the ceramics obtained is uniform and the relative density is above 98% of the theoretical value. Similar to normal $BaTiO_3$ ceramics, successive phase transitions are observed in the 30 nm $BaTiO_3$ ceramics using variable-temperature X-ray diffraction measurements. Furthermore the 30 nm $BaTiO_3$ ceramics reveal ferroelectric properties after being post-annealed at low temperature in O_2 atmosphere, but the phase transition temperature from paraelectric to ferroelectric phase is 10 °C lower than that of a normal bulk sample. The results indicate that dense 30 nm $BaTiO_3$ ceramics retain ferroelectricity above room temperature.

1 Introduction

Size effects in ferroelectric systems have attracted great attention because of their potential application in information technology. Barium titanate ($BaTiO_3$) is a well-known ferroelectric material with high dielectric constant and low losses above room temperature [1, 2]. The effects of grain size on the phase transitions and the ferroelectric properties of $BaTiO_3$ crystals have been studied both theoretically [3] and experimentally [4–12] in recent years. It is well known that bulk $BaTiO_3$ undergoes successive phase transitions with decreasing temperature from paraelectric cubic phase to ferroelectric tetragonal phase (C–T) at ~130 °C, then from ferroelectric tetragonal to another ferroelectric orthorhombic phase (T–O) at ~5 °C, finally from orthorhombic to rhombohedral phase (O–R) at about −80 °C. The ferroelectric properties of $BaTiO_3$ ceramics strongly depend on the grain size, and have a pronounced maximum for a grain size of ~1 μm [4]. Further reducing the grain size leads to a decrease of permittivity. Finally cubic phase will be stabilized at a wide temperature range, leading to the disappearance of the ferroelectricity above room temperature, which hampers the application of the material. Theoretically, the critical grain size for the disappearance of ferroelectricity was predicted to be about 100 nm for $BaTiO_3$ particles [3]. Experimentally, fabricated by spark plasma sintering, Deng et al. [13] and Buscaglia et al. [14] obtained dense $BaTiO_3$ ceramics with grain sizes of 20 and 30 nm, respectively. Using two-step sintering techniques, Wang et al. obtained dense $BaTiO_3$ ceramics with grain sizes of 35 nm [15]. Their results indicated that the ferroelectricity still remains in $BaTiO_3$ nanoceramics. Due to aggregation and exaggerated growth of nanograins, it is difficult to obtain $BaTiO_3$ ceramics with grain size less than 50 nm by conven-

[*] Corresponding author: e-mail: jin@aphy.iphy.ac.cn, Phone: +8610 8264 9163, Fax: +8610 8264 9531

tional methods. So far, there are fewer data for the phase transition and dielectric properties for grain size being less than 50 nm.

In comparison with sintering under ambient pressure, high-pressure sintering could significantly increase the densification and dramatically reduce the growth rate as a result of the suppressed diffusivity [16, 17]. Thus high-pressure sintering is expected to be an ideal approach to obtain dense nanoceramics with extremely small grain size.

In this paper, we report that dense 30 nm $BaTiO_3$ ceramics with homogeneous grain size could be prepared from 10 nm $BaTiO_3$ raw powder using a specified high-pressure sintering route, i.e. a three-step high-pressure sintering method. The 30 nm $BaTiO_3$ ceramics displayed a similar successive phase transition to normal bulk samples as detected using variable-temperature X-ray diffraction. The ferroelectricity was characterized from dielectric measurements.

2 Experimental

The raw material of 10 nm $BaTiO_3$ powder was synthesized by sol–gel processing [18]. In order to eliminate nanograin agglomeration, which happens generally in nanomaterials, a three-step method involving high pressure was adopted to prepare dense uniform $BaTiO_3$ nanoceramics. The first step was to press the raw powder into a pellet uniaxially at 8 MPa at room temperature. In the second step, the pellet was cold pressed under higher pressure, such as 3 GPa, and then it was unloaded and milled into powder. The processed powder was pressed again as in the first step. The second step is crucial to crack the agglomeration and avoid exaggerated grain growth in the following high-pressure sintering. The third step was to process the sample by high-pressure sintering. A pellet of 6 mm in diameter and 2 mm in thickness was wrapped by Ag foil to prevent contamination. The sample set was inserted into a BN spacer tube that was in turn put into a graphite heater. Pyrophyllite was used as the pressure-transmitting medium. High-pressure experiments were carried out in a cubic anvil-type high-pressure apparatus. The sample was first pressurized up to 6 GPa and then heated at 1000 °C, and then kept in the high-pressure and high-temperature state for 5 min. After temperature quenching, the sample was recovered by slowly releasing the pressure.

The samples were characterized using several different techniques. The microstructure was observed using scanning electron microscopy (SEM; XL30-FEG) on fresh fracture surfaces. Grain size was determined by X-ray diffraction (XRD) at room temperature using a Rigaku D/max-2500 diffractometer with Cu K_α radiation. Crystalline structure was investigated using variable-temperature XRD. Dielectric properties in the vicinity of the Curie temperature were measured using an HP 4194A LF impedance analyzer.

3 Results and discussion

Figure 1 shows the microstructure of the sintered bulk. The sample exhibited homogeneous grain size distribution with a 30 nm mean grain size. From XRD, the exact grain size was calculated to be 28 nm from the broadened (111) peak. By means of the Archimedes method, the relative density of $BaTiO_3$ nanoceramics was measured to be above 98% of the theoretical value. If the sintering temperature was enhanced or the sintering period was lengthened, the grain size of $BaTiO_3$ nanoceramics increased. When the sintering temperature reached 1100 °C, the grain size was about 40 nm as shown in Fig. 1b. By comparison, the microstructure of sintered ceramics without the 3 GPa pressing is also shown in Fig. 1c. There are many 'beams' in the $BaTiO_3$ nanoceramics. The details of these 'beams' is described elsewhere [19].

The phase transition of the 30 nm $BaTiO_3$ ceramics was investigated using variable-temperatures XRD. Figure 2a shows XRD patterns of the 30 nm $BaTiO_3$ ceramics at temperatures ranging from –189 to 170 °C. Owing to the presence of high levels of chemisorbed gases, 10 nm raw powder can absorb some impurities such as CO_2, so that there are some barium carbonate impure phases denoted by the arrows in the XRD patterns. Because barium carbonate is not a ferroelectric crystal, it does not affect the ferroelec-

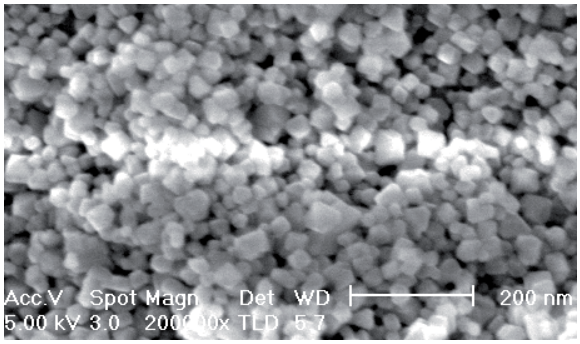

a)

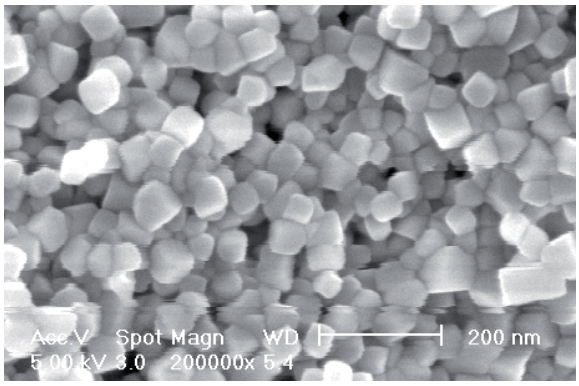

b)

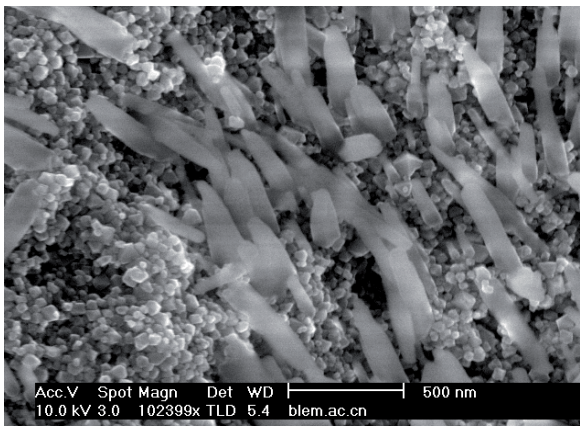

c)

Fig. 1 SEM images of $BaTiO_3$ ceramics: a) three-step high-pressure sintering method at 6 GPa, 1000 °C, 5 min; b) three-step high-pressure sintering method at 6 GPa, 1100 °C, 5 min; c) direct sintering method at 6 GPa, 1000 °C, 5 min.

tricity of barium titanate. Since diffraction peaks cannot be separated accurately due to the marked broadening and overlap when the particle size is reduced to the nanoscale [20], and moreover there are multiphase coexistences in $BaTiO_3$ nanoceramics observed by Raman scattering [13, 15], we only traced the shift tendency of XRD peaks, for example (200)-(002) peaks as shown in Fig. 2b. The peak indexing at room temperature was simply based on the cubic structure with space group Pm3m. In order to compare with normal $BaTiO_3$ ceramic and accordingly explicitly explain the phase transition of the 30 nm $BaTiO_3$ ceramics, we first studied 600 nm $BaTiO_3$ ceramics sintered by the same method, whose original grain size of raw powder is 500 nm. Fig. 2c represents the enlarged XRD patterns of 600 nm $BaTiO_3$ ceramics between $2\theta = 43.5°$ and 46.0° with increasing temperature. The change in trends of the stronger peaks at various temperatures is characterized by the dotted lines in Fig. 2c. The four typical diffraction patterns obviously exhibited the characteristic of cubic, tetragonal, orthorhombic and rhombohedral

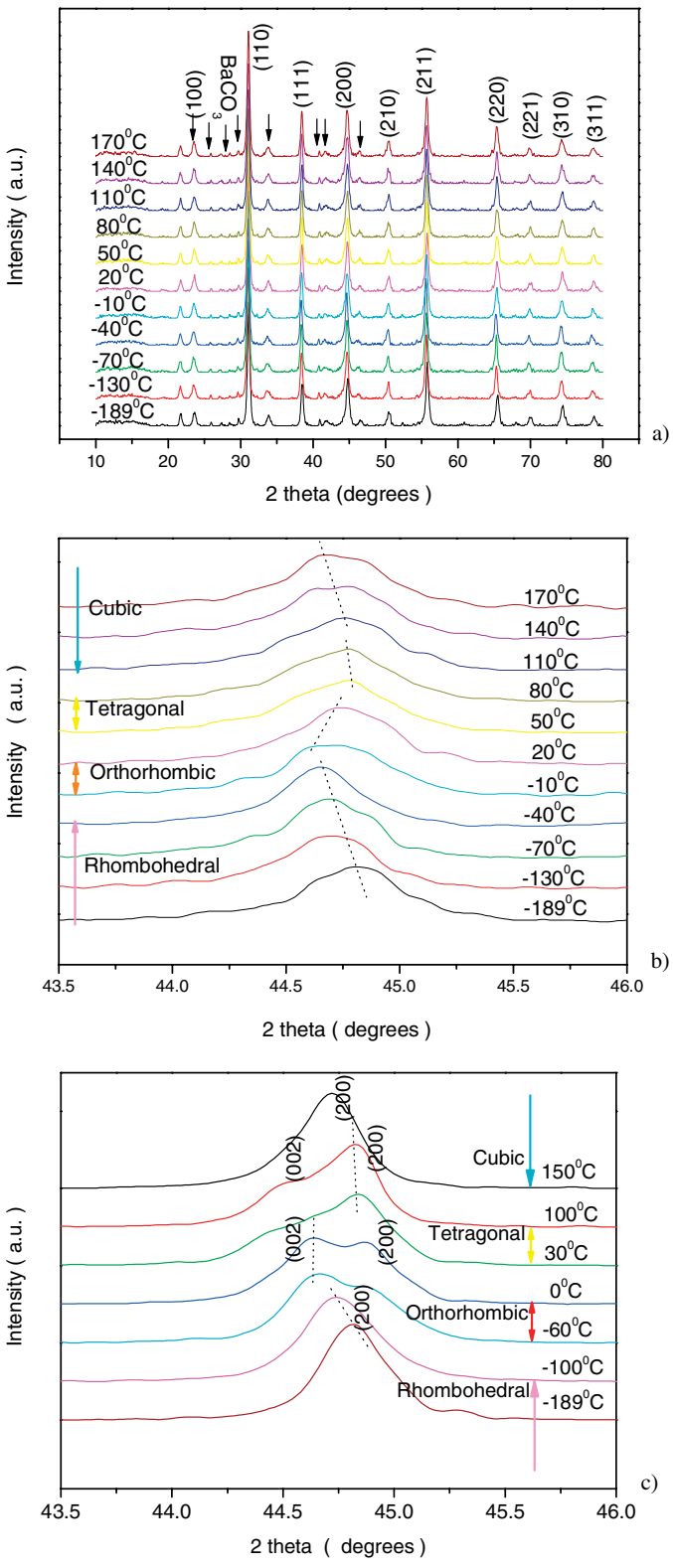

Fig. 2 (online colour at: www.pss-a.com) a) XRD patterns of 30 nm $BaTiO_3$ ceramics at temperatures ranging from −189 to 170 °C. b) Enlarged (200)-(002) XRD peaks of 30 nm $BaTiO_3$ nanoceramics at various temperatures. The changing trends of 2θ value of (200)-(002) peaks at various temperatures are indicated by the dotted lines. c) Enlarged (200)-(002) XRD peaks of 60 nm $BaTiO_3$ ceramics at various temperatures. The changing trends of stronger peaks at various temperatures are indicated by the dotted lines.

Table 1 Phase transition temperature regions of 30 nm, 600 nm and normal $BaTiO_3$ ceramics.

grain size (nm)	T_C (°C)	T_{T-O} (°C)	T_{O-R} (°C)
30	80 – 110	20 – 50	−40 to −10
600	100 – 150	0 – 30	−100 to −60
normal ceramic	130	5	−90

phases, indicating the successive phase transition happened as a function of temperature. Moreover the phase transition temperature intervals are inconsistent with those for normal bulk samples. In contrast to the 600 nm ceramics, the diffraction peaks of the 30 nm $BaTiO_3$ ceramics at various temperatures are very diffuse, but the shift trend of (200)-(002) diffraction peaks with increasing temperature was clear as shown in Fig. 2b, indicating successive phase transitions occurred in the 30 nm $BaTiO_3$ ceramics. Compared with the change of (200)-(002) peaks of 600 nm ceramics, the phase transitions were consequently assigned as from cubic to tetragonal, then to orthorhombic, and to rhombohedral with the decreasing temperature. According to the (200)-(002) peak evolution, the phase transition temperature regions of the 30 nm $BaTiO_3$ ceramics are between 80 and 110 °C for T_C, between 20 and 50 °C for T_{T-O} and between −40 and −10 °C for T_{O-R}. It is obvious that for the 30 nm $BaTiO_3$ ceramics the phase transition temperature from cubic to tetragonal (T_C) shifts to lower temperature while those from tetragonal to orthorhombic (T_{T-O}) and from orthorhombic to rhombohedral (T_{O-R}) shift to higher temperatures compared with the normal $BaTiO_3$ ceramics. Table 1 summarizes the phase transition temperature regions of 30 nm, 600 nm and normal $BaTiO_3$ ceramics.

The temperature dependences of the dielectric constant of the as-prepared and post-annealed 30 nm $BaTiO_3$ ceramics and 600 nm $BaTiO_3$ ceramics at 10 kHz are shown in Fig. 3. There is no obvious dielectric peak for the as-prepared 30 nm $BaTiO_3$ ceramics that may be caused by oxygen vacancies and stress arising from the airproof atmosphere and exterior high pressure in the high-pressure sintering process. The as-prepared 30 nm $BaTiO_3$ ceramics were annealed in O_2 atmosphere at 600 °C for 8 h. The process has little effect on the grain size, but greatly improves dielectric properties. A broadened dielectric peak appeared at 120 °C for the post-annealed 30 nm $BaTiO_3$ ceramics, whose dielectric constant was 1700. In comparison with 600 nm $BaTiO_3$ ceramics, whose broadened dielectric peak appeared at

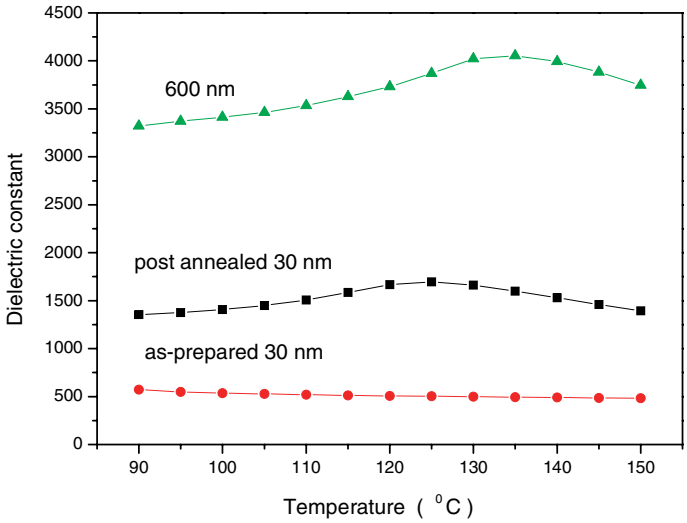

Fig. 3 (online colour at: www.pss-a.com) Temperature dependence of the dielectric constant of as-prepared and post-annealed 30 nm $BaTiO_3$ ceramics, and 600 nm $BaTiO_3$ ceramics at 10 kHz, indicating a ferroelectric phase transition above room temperature in the 30 nm $BaTiO_3$ ceramics.

130 °C, the ferroelectric phase transition temperature was reduced, which is in agreement with the observation from variable-temperature XRD measurements. The dielectric peak indicated that the ferroelectricity still remained, but the dielectric property was strongly depressed in dense 30 nm $BaTiO_3$ ceramics.

It is well known that nanopowders have extremely large specific area and tend to be strongly agglomerated. Although it is easy to break down the soft agglomerates, collapsing hard agglomerates needs larger forces, so the applied pressure must be very high, such as 3 GPa. Using cold isostatic pressing under ultrahigh pressure brings large shearing forces to bear on the nanoparticles, so that plastic deformation occurs, which breaks down the agglomerates.

A progressive reduction of tetragonal distortion with decreasing grain size was found [4, 21]. For the 30 nm $BaTiO_3$ ceramics, the tetragonal distortion of the lattice was evaluated using the Rietveld refinement method to be 1.0058. The low tetragonal distortion leads to a reduced spontaneous polarization and the lowering of the dielectric constant. Also, the lowered relative dielectric constant was explained by nonferroelectric grain boundaries with lower permittivity [21–23]. The values of permittivity and thickness of the grain boundaries were estimated theoretically to be $\varepsilon_r = 100$ and $d = 0.7$ nm, which are in reasonable agreement with the experimental data [23]. Moreover, the fraction of grain boundary volume increases with decreasing grain size. So the total dielectric constant decreases with decreasing grain size.

4 Conclusions

Dense 30 nm $BaTiO_3$ ceramics were fabricated using three-step high-pressure sintering. We investigated the variable-temperature XRD of 30 nm $BaTiO_3$ ceramics at temperatures ranging from –189 to 170 °C. The results indicated that the successive phase transitions occurred in 30 nm $BaTiO_3$ ceramics when the temperature increased. After post-annealing in O_2 for 8 h at 600 °C, the 30 nm $BaTiO_3$ ceramics revealed the feroelectric phase transition. The result confirmed that, although the dielectric properties are dependent on the grain size, the ferroelectricity still persisted in the dense 30 nm $BaTiO_3$ ceramics.

Acknowledgement This work was supported by the Ministry of Sciences and Technology of China through research project 2002B613301.

References

[1] M. E. Lines and A. M. Glass, Principles and Applications of Ferroelectrics and Related Materials (Clarendon, Oxford, 1977).
[2] E. K. Akdogan, M. R. Leonard, and A. Safari, in: Handbook of Low and High Dielectric Constant Materials for Applications, Vol. 2, edited by H. S. Nalwa (Academic Press, New York, 1999).
[3] W. L. Zhong, Y. G. Wang, P. L. Zhang, and B. D. Qu, Phys. Rev. B **50**, 698 (1994).
[4] G. Arit, D. Hennings, and G. D. With, J. Appl. Phys. **58**, 1619 (1985).
[5] F. S. Yen, H. Hsing-H, and C. Y. Hwei, Jpn. J. Appl. Phys. **34**, 6149 (1995).
[6] S. Stefan and E. H. Friedrich, Solid State Commun. **91**, 883 (1994).
[7] M. H. Frey and D. A. Payne, Phys. Rev. B **54**, 3158 (1996).
[8] K. Kinoshita and A. Yamaji, J. Appl. Phys. **47**, 371 (1976).
[9] B. Jaffe, W. R. Cook, and H. L. Jaffe, Piezoelectric Ceramics (Academic Press, London, 1971).
[10] K. Uchino, E. Sadanaga, and T. Hirose, J. Am. Ceram. Soc. **72**, 1555 (1989).
[11] B. D. Bruce, V. R. Eric, and N. Janusz, J. Am. Ceram. Soc. **77**, 3186 (1994).
[12] Y. Kuroiwa, S. Aoyagi, A. Sawada, and H. Ikawa, J. Therm. Anal. Cal. **69**, 933 (2002).
[13] X. Y. Deng, X. H. Wang, H. Wen, A. G. Kang, Z. L. Gui, and L. T. Li, J. Am. Ceram. Soc. **89**, 1059 (2006).
[14] M. T. Buscaglia, M. Viviani, V. Buscaglia, L. Mitoseriu, A. Testino, P. Nanni, Z. Zhao, M. Nygren, C. Harnagea, D. Piazza, and C. Galassi, Phys. Rev. B **73**, 064114 (2006).
[15] X. H. Wang, X. Y. Deng, H. L. Bai, H. Zhou, W. G. Qu, L. T. Li, and I. W. Chen, J. Am. Ceram. Soc. **89**, 438 (2006).
[16] G. Skandan, Nanostruct. Mater. **5**, 111 (1995).
[17] S.-C. Liao, Y.-J. Chen, B. H. Kear, and W. E. Mayo, Nanostruct. Mater. **10**, 1063 (1998).
[18] B. R. Li, X. H. Wang, L. T. Li, and H. Zhou, Mater. Chem. Phys. **78**, 292 (2002).

[19] C. J. Xiao, H. Yang, R. C. Yu, F. Y. Li, Z. H. Chi, C. Q. Jin, X. H. Wang, and L. T. Li, submitted.
[20] D. Fu, H. Suzuki, and K. Ishikawa, Phys. Rev. B **62**, 3125 (2000).
[21] Z. Zhao, V. Buscaglia, M. Viviani, M. T. Buscaglia, L. Mitoseriu, A. Testino, M. Nygren, M. Johnsson, and P. Nanni, Phys. Rev. B **70**, 024107 (2004).
[22] M. H. Frey, Z. Xu, P. Han, and D. A. Payne, Ferroelectrics **206/207**, 337 (1998).
[23] A. Yu. Emelyanov, N. A. Pertsev, S. Hoffmann-Eifert, U. Bfttger, and R. Waser, J. Electroceram. **9**, 5 (2002).

